frontiers in Marine Science

ORIGINAL RESEARCH
published: 27 January 2022
doi: 10.3389/fmars.2022.812839

High-Resolution Dynamics of Hydrogen Peroxide on the Surface of Scleractinian Corals in Relation to Photosynthesis and Feeding

Sara Ousley[1,2], Dirk de Beer[2], Sonia Bejarano[1] and Arjun Chennu[1,2]**

[1] Leibniz Centre for Tropical Marine Research, Bremen, Germany, [2] Max Planck Institute for Marine Microbiology, Bremen, Germany

We developed and used a microsensor to measure fast (<1 s) dynamics of hydrogen peroxide (H_2O_2) on the polyp tissue of two scleractinian coral species (*Stylophora pistillata* and *Pocillopora damicornis*) under manipulations of illumination, photosynthesis, and feeding activity. Our real-time tracking of H_2O_2 concentrations on the coral tissue revealed rapid changes with peaks of up to 60 μM. We observed bursts of H_2O_2 release, lasting seconds to minutes, with rapid increase and decrease of surficial H_2O_2 levels at rates up to 15 μM s^{-1}. We found that the H_2O_2 levels on the polyp surface are enhanced by oxygenic photosynthesis and feeding, whereas H_2O_2 bursts occurred randomly, independently from photosynthesis. Feeding resulted in a threefold increase of baseline H_2O_2 levels and was accompanied by H_2O_2 bursts, suggesting that the coral host is the source of the bursts. Our study reveals that H_2O_2 levels at the surface of coral polyps are much higher and more dynamic than previously reported, and that bursts are a regular feature of the H_2O_2 dynamics in the coral holobiont.

Keywords: reactive oxygen species, hydrogen peroxide, corals, microsensors, oxidative bursts, photosynthesis, coral feeding, chemical ecology

OPEN ACCESS

Edited by:
Daniel Wangpraseurt, University of California, San Diego, United States

Reviewed by:
Anthony William Larkum, University of Technology Sydney, Australia
Daniel Aagren Nielsen, University of Technology Sydney, Australia

****Correspondence:***
Sara Ousley
sara.whitaker.ous@gmail.com
Arjun Chennu
arjun.chennu@leibniz-zmt.de

Specialty section:
This article was submitted to Coral Reef Research, a section of the journal Frontiers in Marine Science

Received: *11 November 2021*
Accepted: *05 January 2022*
Published: *27 January 2022*

Citation:
Ousley S, de Beer D, Bejarano S and Chennu A (2022) High-Resolution Dynamics of Hydrogen Peroxide on the Surface of Scleractinian Corals in Relation to Photosynthesis and Feeding. Front. Mar. Sci. 9:812839. doi: 10.3389/fmars.2022.812839

INTRODUCTION

Reactive oxygen species (ROS), such as hydrogen peroxide (H_2O_2) and superoxide anion ($O_2^{\cdot -}$), are toxic at high levels, but also function as signaling molecules essential for the integrity of homeostasis and health of cells in nearly all eukaryotic organisms (D'Autréaux and Toledano, 2007; Nathan and Cunningham-Bussel, 2013). Intracellular ROS production occurs primarily in mitochondria, chloroplasts and membrane-bound peroxisomes through specialized mechanisms in the respiratory burst oxidase homologs, such as NADPH oxidase enzymes (Suzuki et al., 2011). ROS are produced under normal growth conditions, but stress conditions trigger elevated concentrations and production rates (Mittler, 2002), causing deleterious effects to vital cell organelles (Lesser, 2006). As high levels of ROS can cause oxidative damage, organisms tightly regulate internal levels of ROS through antioxidant activity of enzymes such as superoxide dismutase, catalase, and ascorbate peroxidase (Fridovich, 1998; Mittler, 2002). However, the occurrence of extracellular or external ROS has recently been recognized as a remarkably widespread biochemical, geochemical, and physiological pathway in marine biota and ecosystems (Sutherland et al., 2020; Hansel and Diaz, 2021).

Scleractinian corals, the primary reef-building organisms across shallow tropical coasts, are obligate hosts of microbial *Symbiodiniaceae* algae which live within the coral's transparent soft tissue in an intricate symbiosis involving the exchange of nutrients and metabolites (Stanley and van de Schootbrugge, 2009). This symbiosis is the "engine of the reef" and is at the heart of the evolutionary and ecological success of corals (Roth, 2014), which as sessile organisms with limited mobility, must interact chemically with predators, prey, competitors, and microbial pathogens (Bakus, 1981; Pawlik, 1993; Paul and Puglisi, 2004). Since ROS are an inevitable consequence of aerobic or photosynthetic life, they are important side-products of metabolic activity produced by various components of the coral holobiont, consisting of the coral polyp, the endosymbiotic algae, and the endosymbiotic and epibiotic bacteria (Saragosti et al., 2010; Armoza-Zvuloni et al., 2016a; Zhang et al., 2016). Light and heat stress can cause damage to the photosystem machinery of *Symbiodiniaceae* cells, resulting in elevated concentrations of photochemically derived ROS within host tissues (Downs et al., 2002; Weis, 2008; Diaz et al., 2016). This overproduction of ROS and the resulting oxidative stress has been hypothesized to lead to the breakdown of host-algae symbiosis during coral bleaching (Downs et al., 2002; Lesser, 2011).

The level of reactive oxygen species in coral tissues has been associated with thermal tolerance, pathogen defense and prey acquisition (Armoza-Zvuloni et al., 2016a,b). Within the coral holobiont, superoxide is generated through multiple mechanisms, including the photosynthetic activity of *Symbiodiniaceae*. Given the limited ability of superoxide to be transported across cell membranes, the most likely sources of extracellular superoxide are epibiotic microbes and the coral's epithelial cells (Zhang et al., 2016). NADPH oxidase enzymes produce extracellular superoxide, while superoxide dismutase rapidly degrades superoxide to H_2O_2 (Hansel and Diaz, 2021). External superoxide levels as high as 120 nM (seawater level is typically pM–nM) were found near coral tissue (Saragosti et al., 2010; Diaz et al., 2016). Unlike superoxide, H_2O_2 can diffuse across cell membranes unhindered and therefore external H_2O_2 levels on coral tissue can be influenced by both intracellular processes such as photosynthesis as well as extracellular processes, such as surficial regulation of antioxidant enzymes (Levy, 2006). Superoxide degradation by superoxide dismutase typically results in the formation of H_2O_2, which means that extracellular superoxide is a potential source of external H_2O_2. Corals regulate H_2O_2 levels at their tissue surface by releasing H_2O_2 and quenching by enzymes (such as ascorbate, peroxidase, catalase) which degrade H_2O_2 to water (Shaked and Armoza-Zvuloni, 2013; Armoza-Zvuloni and Shaked, 2014). Thus, both the coral and the endosymbiotic algae are implicated in the regulation of external H_2O_2 levels.

Knowledge on the dynamics of external H_2O_2 in live corals comes predominantly from studies quantifying H_2O_2 or superoxide concentrations in the ambient water sampled from the vicinity of the coral tissue (Saragosti et al., 2010; Armoza-Zvuloni and Shaked, 2014; Diaz et al., 2016). Despite the limited spatial and temporal resolution of this technique, spatially localized (10 mm^2) elevations of external H_2O_2 reaching up to 1 μM have been observed (Armoza-Zvuloni et al., 2016a; Szabó et al., 2020). Conclusions about external H_2O_2 mainly being "produced by algae through pathways other than photosynthesis" invite further investigation (Armoza-Zvuloni and Shaked, 2014).

Previous indirect estimations suggest H_2O_2 concentration, denoted as $[H_2O_2]$, of ∼20 μM within the mass boundary layer (MBL) at the coral tissue (Armoza-Zvuloni et al., 2016a). Another study reported a concentration change of up to 140 nM of external H_2O_2 over 4–6 min in response to feeding or physical stimuli (Armoza-Zvuloni et al., 2016b). Quantifying ROS levels in the water surrounding corals provides an indirect, and likely inaccurate, estimate of $[H_2O_2]$ within the coral MBL due to unintended sample dilution and limited temporal resolution of measurements. There is growing recognition of the importance of polyp-scale mechanisms of ROS control in the photobiology and physiology of the coral holobiont to understand coral bleaching, thermal resilience and response to disease (Smith et al., 2005; Mydlarz and Jacobs, 2006; Tchernov et al., 2011; McGinty et al., 2012; Gustafsson et al., 2013, 2014; Krueger et al., 2015; Montilla et al., 2016; Baird et al., 2018; Szabó et al., 2020). Therefore, improved *in situ* sensing technologies are necessary to quantify ROS on live coral polyps with improved temporal and spatial resolutions (Hansel and Diaz, 2021).

In this study, we developed a microsensor to measure H_2O_2 concentrations and applied it toward the fine-scale study of H_2O_2 dynamics at the surface of scleractinian coral polyps. We present the details of the sensor design and construction and its first application for studies on live coral tissue. Using two important reef-building species (*Stylophora pistillata* and *Pocillopora damicornis*) we conducted laboratory experiments to resolve the following questions:

1. What are the characteristics of the MBL and H_2O_2 dynamics at the coral polyp surface?
2. How is the H_2O_2 level at the polyp surface affected by changes in light intensity and photoactivity in the coral holobiont?
3. How does the feeding behavior of corals affect the surficial H_2O_2 level, and is H_2O_2 used in prey capture?
4. What are the sources, sinks, and processes within the coral holobiont that influence the level of H_2O_2 on the polyp surface?

MATERIALS AND METHODS

H_2O_2 Sensor Design and Calibration

The design of the H_2O_2 microsensor (**Figure 1A**) was an adaptation of a previously described glucose microsensor (Cronenberg et al., 1991). A platinum wire (99.99%, hardened, 50 μm diameter; Goodfellow Cambridge Ltd., Huntingdon, United Kingdom) was coated with a glass covering. The tip of the covering was opened with tweezers and the etched by applying a 2 V alternating current in saturated KCN to obtain a tip diameter of 10–30 μm. The platinum wire was etched back approximately 15 μm from the tip, and then plated in 8% platinum chloride ($PtCl_4$) in distilled water for approximately 10 min until a sponge

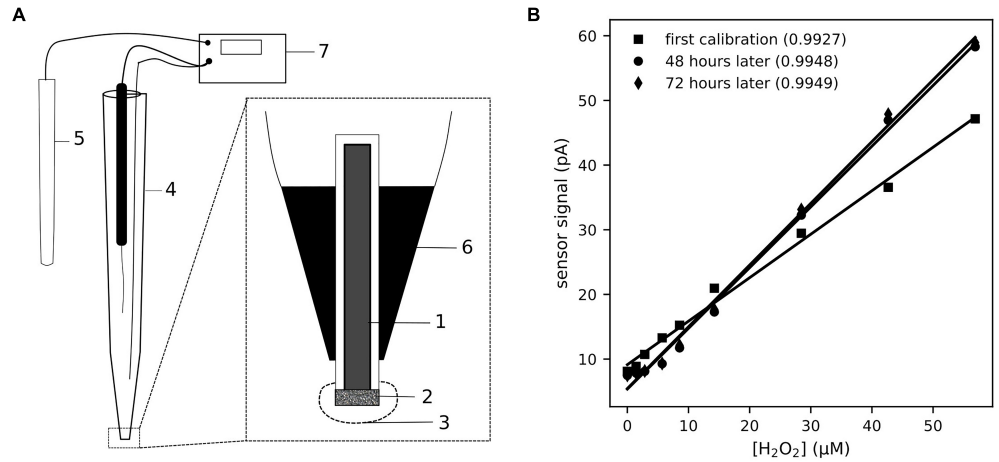

FIGURE 1 | The schematic **(A)** shows the design and construction of the H_2O_2 sensor used for this study. The Pt-electrode (1) was coated with a Pt-sponge (2) and the tip of the sensor was covered with a cross-linked BSA coating (3). The electrode was insulated in a glass capillary (4), filled with 3 M KCl, and connected with a silver wire to the reference (5). The electrode is fixed in the capillary by epoxy (6) and connected to the amplifier (7) by a coax cable. The electrical potential between the reference and Pt-electrode was set to a polarization voltage of 0.7 V, as this is the anodic potential for H_2O_2 oxidation on Pt surfaces. The sensor signal **(B)** responded linearly to increasing [H_2O_2], in the range 0–50 μM, added to the seawater medium. The response of the sensor showed some drift over a few days of operation, but remained linear (coefficient of determination of the linear fit provided in the legend).

of porous platinum was formed that extended 5–10 μm from the tip. The tip was then coated with cross-linked bovine serum albumin (BSA). Ten microliters of 50% glutaraldehyde was added to 1 mL of 10% BSA in 50 mM phosphate buffer (pH 7), vortexed intensively for 3 s. The mixture can be used as long as it is syrupy, but hardens within a few minutes. Under microscopic guidance the tip of the etched platinum wire was dipped shortly in the BSA mixture and then left to dry till a thin, ceramic-like layer of cross-linked BSA formed on the tip. This layer forms a molecular sieve that creates a constant diffusion barrier and reduces the stirring sensitivity.

An outer glass capillary was made with a tip opening 10 μm larger than the coated platinum wire, with the final tip diameter ranging from 25 to 50 μm. The platinum wire was brought into the outer capillary, so that it stuck out 300 μm. The platinum wire was fixed to the capillary with a drop of UV-hardening epoxy glue, carefully avoiding the tip. A silver wire was inserted inside the glass capillary and together with the platinum wire glued to the outer capillary. The outer capillary was filled with 3 M KCl, and the silver wire connected to a calomel reference, to shield the microsensor from noise.

The sensor was connected with a coaxial cable and set to a potential of +0.7 V against the calomel reference. The sensor-reference couple was placed in a stirred beaker of seawater and left to stabilize until baseline signal did not change and the only signal fluctuations observed was due to noise, which can take several hours.

The anodic reaction of H_2O_2 on the Pt surface (Hall et al., 1998), upon applying an electric potential (+0.7 V) is:

$$H_2O_2 \rightleftharpoons O_2 + 2H^+ + 2e^- \quad (1)$$

Clark-type O_2 microsensors were constructed and calibrated as previously described (Revsbech and Jørgensen, 1986).

The signal from both O_2 and H_2O_2 sensors was read out by connecting the coaxial and reference cables to a custom-built amperometer, from which the amplified signals were recorded after digitization on a connected computer.

Calibrations of H_2O_2 sensors were performed in a glass beaker placed inside the experimental aquarium using seawater from the coral holding tanks at the MAREE aquarium facility of the Leibniz Centre for Tropical Marine Research. Continuous mixing during calibrations was maintained by a magnetic stirrer placed under the aquarium. Aliquots of 3% w/v H_2O_2 stock solution were added stepwise and the signals were recorded. As the calibrations were performed in the experimental aquarium with live corals, it was not possible to measure a "true zero" signal by adding H_2O_2 quenching enzymes. So our calibration procedure provides [H_2O_2] relative to the value of ambient seawater, which is typically 100 nM (Shaked and Armoza-Zvuloni, 2013). Some negative values of [H_2O_2] were found in the calibrated signal during coral experiments. In such cases, to maintain consistency in the time series, all values in the series were adjusted so that the lowest value of [H_2O_2] was zero. Measurements that did not extend to negative concentrations were not changed.

Analyte Cross-Sensitivity

Cross-sensitivity was tested by separately adding aliquots of acetate, formate, ascorbate, nitrite, nitrate, and nitric oxide to the calibration chamber with the H_2O_2 sensor. The sensor signal for each concentration level for each tested analyte was used to estimate the sensitivity (pA μM^{-1}) through a linear regression. All analytes, with exception of nitric oxide, were calibrated with two H_2O_2 sensors. Nitric oxide was tested in both anoxic and oxic seawater with one H_2O_2 sensor. The cross-sensitivity of each analyte was assessed as the ratio (%) between the sensitivity to the analyte and sensitivity to H_2O_2.

Coral Experiments

Coral Microsensing Setup

Corals were held in filtered seawater within a glass aquarium (40 cm × 25 cm × 15 cm) with a flow-through circulation from an external reservoir, totaling 33 L. The water originated from the MAREE holding tank of the coral specimens and was exchanged entirely every week. The temperature was kept at 25.5°C, under broadband illumination of a 12 h-illuminated diel cycle, except when light levels were manipulated for experiments.

The microsensor setup consisted of manual and motorized micromanipulators, which provide precise position information, and computer-controlled data acquisition (NI-DAQmx; National Instruments, Austin, TX, United States). Microsensor recordings were either made by spatial profiling, i.e., recording sensor signals along with position of the sensor tip at various distances from the coral tissue, or by temporal monitoring, i.e., recording sensor signals without moving the sensor tip.

The sensor tips were gently brought into contact with the edge of the polyp mouth (**Figure 2A**), guided by binoculars and micromanipulators. If contact with the sensor caused polyp retraction, experiments proceeded only after the polyp had re-extended. All the monitoring runs performed in the various experiments contained time-stamped recordings of operator comments along with the microsensor signals.

Coral Handling

Healthy fragments of adult branching corals *S. pistillata* and *P. damicornis* used for this study, were sourced from the MAREE aquarium facility of the Leibniz Centre for Tropical Marine Research and originally reproduced and reared in captivity (Hagenbeck Zoo, Hamburg, Germany and Royal Burgers' Zoo, Arnhem, Netherlands). The fragments were maintained at 25.5 ± 0.3°C and 35 ± 2 ppt salinity.

The coral fragments were transported to the experimental aquarium at the Max Planck Institute for Marine Microbiology (∼15 min), and allowed to acclimate for ∼3 h before any measurements were performed. The coral fragments were kept in the experimental aquarium maximally 5 days before being returned to the MAREE facility.

Light and Photosynthesis Manipulation

H_2O_2 and O_2 levels were obtained from simultaneous microsensor measurements on adjacent polyps. Illumination was provided with a halogen lamp with double swan necks (KL1500; Schott AG, Mainz, Germany). The incident light level was adjusted using the lamp's power setting and measured near the monitored polyp using a scalar irradiance meter (OSL-100; Biospherical Instruments, San Diego, CA, United States).

Experiments related to photosynthesis (Light + PS) were conducted by monitoring H_2O_2 and O_2 levels during step-changes of incident light level, with each step lasting 5 min. Measurements were conducted on 16 polyps from 4 fragments of *S. pistillata* (n = 8 polyps) and 4 fragments of *P. damicornis* (n = 8 polyps), ranging from 1 to 3 polyps per fragment. For experiments that eliminated photosynthesis (Light − PS), DCMU (3-(3,4-dichlorophenyl)-1,1-dimethylurea), a specific inhibitor that blocks the plastoquinone pool in photosystem II was added (2.5–7 μM final concentration). As DCMU sticks strongly to surfaces, the inhibition experiments were done in a 1 L beaker. Since DCMU is dissolved in 90% ethanol, the effect of ethanol without DCMU was also checked. Measurements were conducted on 7 polyps from 2 fragments of *S. pistillata* and 10 polyps from 3 fragments of *P. damicornis*.

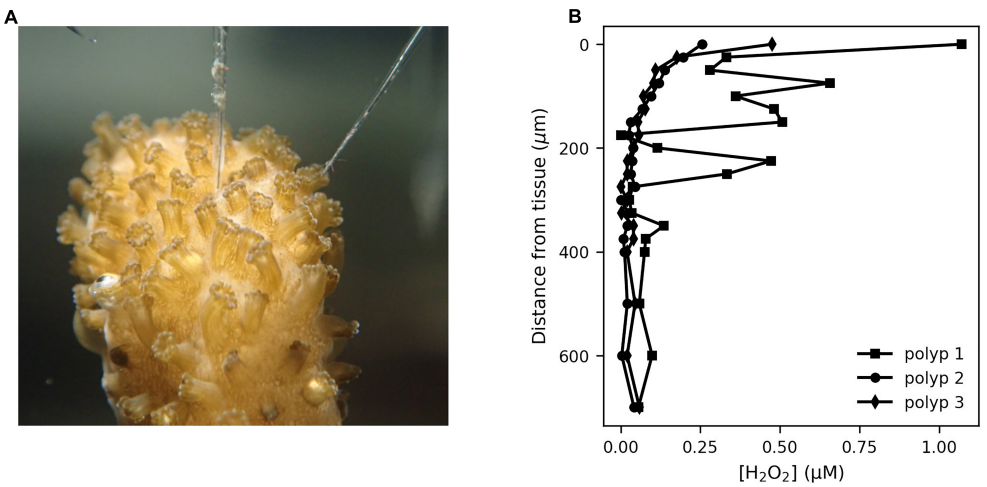

FIGURE 2 | The mass boundary layer around coral polyps was assessed using H_2O_2 and O_2 microsensors. The sensor tip was brought gently in contact with the polyp entrance for either coral species *S. pistillata* **(A)** and *P. damicornis*, and concentrations recorded at increasing distances from the tissue under an illumination of ∼240 μmol m^{-2} s^{-1}. Two types of [H_2O_2] concentration profiles (examples from *P. damicornis* in **B**) were observed, with some profiles (polyp 2 and 3) showing a smooth gradient from an elevated [H_2O_2] (0.3–0.6 μM) to the ambient seawater level over a distance of 200–300 μm. Some profiles (polyp 1) showed a fluctuating signal in the mass boundary layer, indicating active flow induced by cilia on the polyp surface. Photo credit: Sara Ousley.

Monitoring H_2O_2 During Feeding

H_2O_2 dynamics at the coral tissue were measured before and after prey capture. *Artemia salina* cysts were incubated under high aeration and low light in seawater (28°C, 25 ppt salinity) and hatched nauplii were collected the next day. After monitoring the peroxide levels on a polyp, the sensor tip was moved away from the polyp and the hatched nauplii were added to the beaker. After the monitored polyp captured a nauplius, the peroxide sensor tip was carefully brought back to the polyp and peroxide monitoring was resumed. Measurements were conducted on two polyps of each species.

The effect of H_2O_2 on *A. salina* nauplii was tested by exposing 1-day old nauplii to various concentrations of H_2O_2 (0, 5, 10, 20, 50, and 100 μM) in seawater. The health and activity of nauplii was assessed visually, through observations of active swimming in response to light, before H_2O_2 addition, and after 5, 30, 60, and 120 min, and 24 h.

Analysis of H_2O_2 Dynamics

The monitoring runs were grouped into three experimental categories: "Light + PS" for the variations of incident light without DCMU, "Light − PS" for the variations in incident light with DCMU addition and "Feeding" for the measurements during active feeding. Within each category, the monitoring runs were visually inspected to identify various types of H_2O_2 dynamics observed such as spikes, linear ramps and bursts of peroxide. As the spikes were considered an artifact (see section "Results"), we focused our analysis on H_2O_2 ramps and bursts.

In the linear ramps, the rates of change of $[H_2O_2]$ and $[O_2]$ upon a change in incident light level were calculated in the first 30 s. The rates of change of $[H_2O_2]$ and $[O_2]$ for each coral species were related with a simple linear model with zero intercept. The ratio between the rates of change is an indication of the sensitivity of external H_2O_2 level to changes in O_2 cycling.

Bursts were identified as rapid increases of $[H_2O_2]$ from some baseline level, sometimes sustained for a few seconds or minutes, followed by a return to lower $[H_2O_2]$ levels. To focus on biologically induced H_2O_2 signals, we only considered bursts where the amplitude of change in $[H_2O_2]$ was greater than 1 μM and the duration was greater than 10 s. For each burst, a "burst strength" was calculated as the area under the $[H_2O_2]$ curve over time, with units μM s. The burst strength therefore includes the baseline level as well as the short-lived increase and decrease of H_2O_2. The burst strength represents the integral $[H_2O_2]$ within the MBL of the polyp over the duration that the burst lasted. For each coral species, the burst strength between experimental treatments was compared for difference in the mean values using Welch's unequal variances *t*-test.

RESULTS

Characteristics of H_2O_2 Microsensor

The step-wise calibration procedure produced highly linear responses of the sensor signal to $[H_2O_2]$, showing only minor drift in sensitivity over several days (**Figure 1B**). Each constructed sensor had a different sensitivity. Sensors with noise level (standard deviation of the signal in seawater) <200 nM were used for measurements on corals. The sensors responded rapidly to H_2O_2, with a 90% response time of <2 s. The selectivity of the sensor in measuring H_2O_2 was generally good (**Table 1**), with no cross-sensitivity observed for acetate and nitrate, and minor cross-sensitivity to formate and nitrite under high concentrations. The cross-sensitivity to nitric oxide and ascorbate was significant.

H_2O_2 Dynamics and Photosynthesis

H_2O_2 profiling of the polyp MBL showed variable results (**Figure 2**), with either smooth profiles and a MBL thickness of 100–200 μm, or a more irregular profile with a MBL thickness of 500 μm. Monitoring $[H_2O_2]$ dynamics in the MBL showed three signal types. Firstly, an immediate sharp peak appeared consistently (**Figure 3A**) upon first contact between sensor tip and coral tissue. These sharp peaks occurred within 300 ms and were followed by a relaxation over 1–2 s to previous levels. These peaks were due to a mechanical effect on the sensor from contact with a surface, possibly due to a piezoelectrical effect and were not further analyzed. The second type of signal was H_2O_2 bursts that followed slower and smoother dynamics (**Figure 3B** and **Supplementary Figures 1, 2**). A third signal type was linear ramps (**Figure 3C**) of $[H_2O_2]$ increase or decrease, which occurred immediately after the incident light level was changed. We considered the ramps and bursts to be biologically induced H_2O_2 dynamics at the coral tissue.

TABLE 1 | The cross-sensitivity of the H_2O_2 sensor to a number of analytes was tested.

Analyte	Tested range (μM)	Sensitivity to analyte (pA μM^{-1})	Sensitivity to H_2O_2 (pA μM^{-1})	Interference (%)
Acetate	1–1916	0	1.4–7.8	0
Formate	1.2–2355	1×10^{-3}	1.4–7.8	<0.1
Nitrate	0.9–1876	0	1.4–7.8	0
Nitrite	1.2–2315	0.03–0.08	1.4–7.8	1–2.5
Nitric oxide (anoxic water)	0.2–6	2.1	4.4	49
Nitric oxide (oxic water)	0.2–2.6	2.8	4.4	63
Ascorbate	0.4–834	0.6–6.5	1.4–7.8	41–83

Each analyte was tested through step-wise additions to seawater, with no H_2O_2 added, and the response of the sensor as apparent $[H_2O_2]$ was recorded. Sensor sensitivity is denoted in pA μM^{-1}. Analyte interference (%) = (analyte sensitivity/H_2O_2 sensitivity) × 100. If two sensors were tested, we report a range of sensitivity and interference.

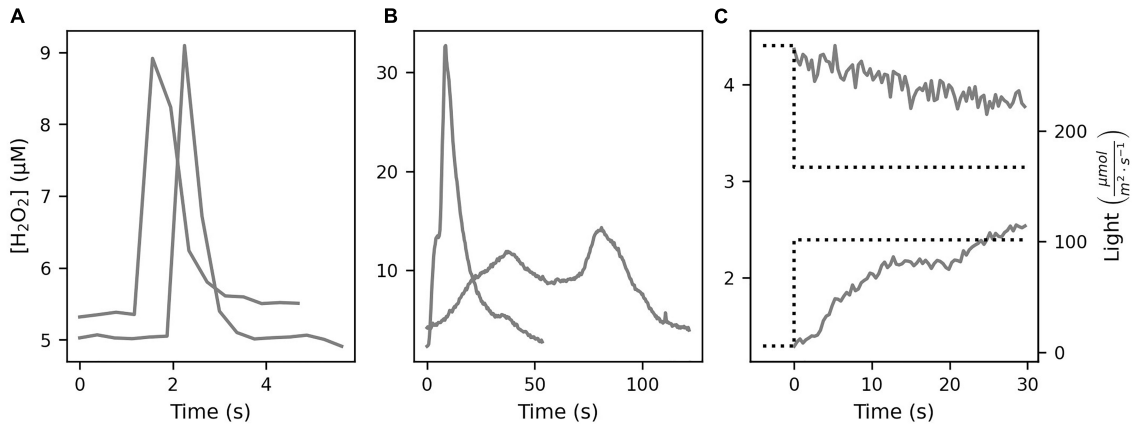

FIGURE 3 | The inference of sensor signals observed during monitoring measurements on coral polyp surface required consideration of the temporal extent and shape of the H_2O_2 signal. Three types of rapid changes of H_2O_2 levels were observed. **(A)** Sharp signal increase within milliseconds followed by a relaxation over 1–5 s, presumed to be a mechanical effect of touching the coral surface with the sensor. **(B)** H_2O_2 "bursts" showed stronger but slower increases, sustained for several seconds or minutes, before returning to lower H_2O_2 levels. **(C)** Step increase or decrease in the incident light (dotted line) induced a corresponding "ramp" of H_2O_2 increase or decrease. Note the different scales of the time and $[H_2O_2]$ axes.

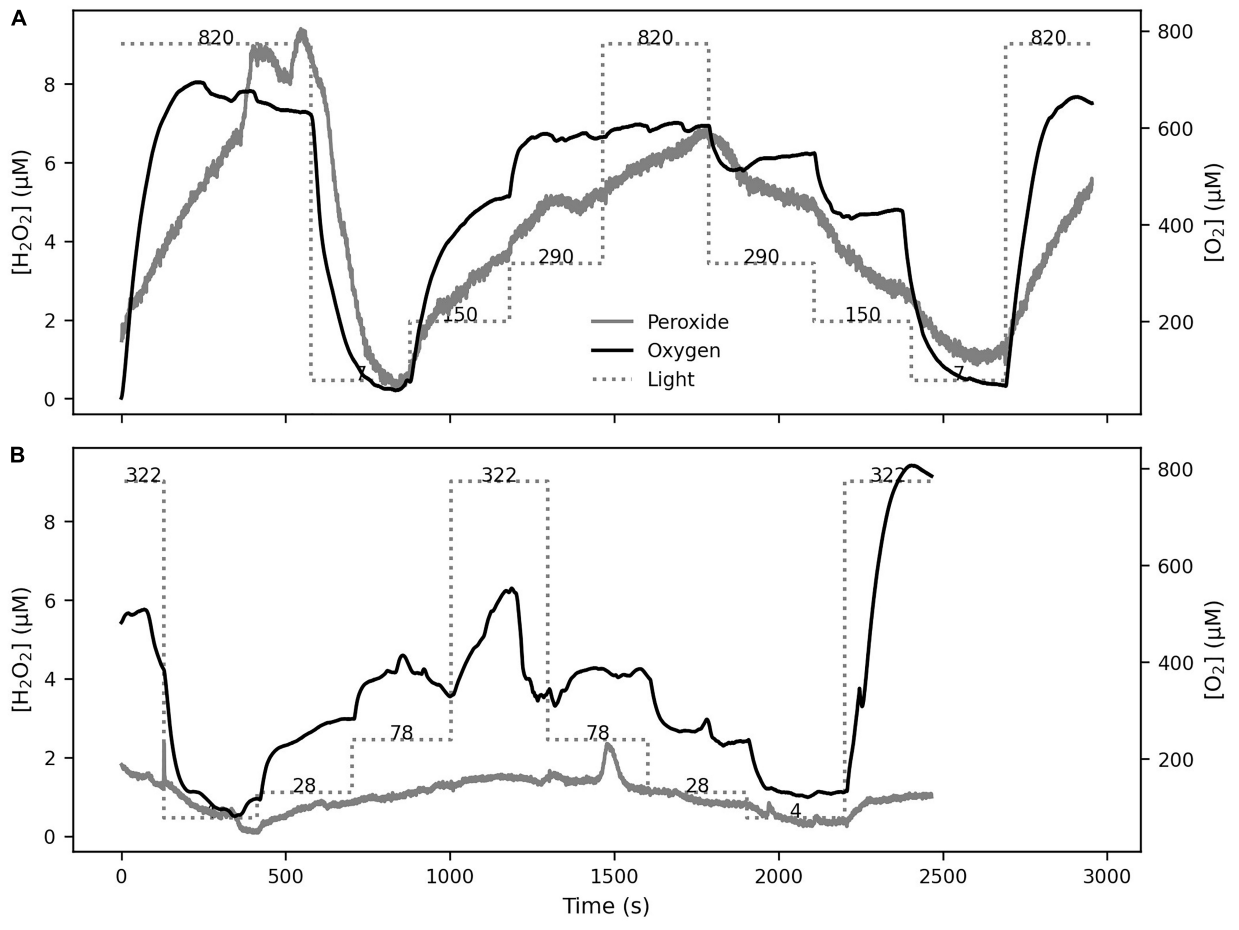

FIGURE 4 | The response of $[O_2]$ and $[H_2O_2]$ on coral tissue was studied under 5-min step-wise changes in illumination levels in *S. pistillata* **(A)** and *P. damicornis* **(B)**. The incident light levels (in µmol m^{-2} s^{-1}) are shown on the *Light* line in both panels. The $[O_2]$ level, driven by photosynthesis, followed the light levels in both species as expected. The $[H_2O_2]$ level also followed similar dynamics, with the notable occurrence of a H_2O_2 burst during a period of constant light level (seen at ~1500 s in **B**).

The $[O_2]$ at the polyp surface were tightly coupled with the incident light level (**Figure 4**). Increasing light levels produced increases in $[O_2]$ (up to twofold air saturation), and decreasing light levels reduced $[O_2]$. The H_2O_2 dynamics were also closely linked to the light levels, with $[H_2O_2]$ values reaching up to 10 μM.

Increases or decreases in incident light produced corresponding positive or negative ramps of $[H_2O_2]$ and $[O_2]$ in both coral species (**Figure 3C**). The absolute rates of $d[H_2O_2]/dt$ in the first 30 s in *S. pistillata* and *P. damicornis* were 0.2–191.4 nM s^{-1} (n = 35) and 1.2–194.6 nM s^{-1} (n = 45), respectively (**Figure 5**). The corresponding ranges for $d[O_2]/dt$ rates were 0.02–16.4 and 0.2–13.0 μM s^{-1}. The ratio of $d[H_2O_2]/dt$ rate to $d[O_2]/dt$ rate was in the range 0.01–2.96% (median = 0.66%) for *S. pistillata* and 0.03–10.61% (median = 1.75%) for *P. damicornis*. Additionally, we observed higher rate variability in *P. damicornis* compared to *S. pistillata* (**Figures 5C,D**).

Upon addition of DCMU, the dynamics of O_2 and H_2O_2 in response to incident light levels was eliminated. This indicates that DCMU addition was effective in inhibiting photosynthesis in the coral polyps without interference from ethanol (**Supplementary Figure 3**). Bursts occurred frequently during all experimental manipulations in both species, independent of light level, oxygen concentration or photosynthetic activity. During light manipulations, a series of H_2O_2 bursts occurred even when the light levels were constant (**Figure 6A**). Bursts were also observed when photosynthesis was inhibited with DCMU (**Supplementary Figures 4, 5**) and light levels were constant, either high or low, and the oxygen at the coral tissue depleted (**Figures 6B,C**). In general, the timing of the bursts was unpredictable and showed variable rates of $[H_2O_2]$ change, with 99 percentile value of 5.25 μM s^{-1} and a maximum of 15.02 μM s^{-1}.

H_2O_2 Dynamics During Feeding

$[H_2O_2]$ on the coral polyp was stable before prey capture, at a level specific to each polyp ranging from 1.8 to 10.1 μM (**Figure 7**). Monitoring of $[H_2O_2]$ on the coral polyp was resumed within 60–100 s of prey capture. The baseline $[H_2O_2]$ was elevated to 8–20 μM during prey handling (**Figures 7A,B**). During prey handling, the amplitude of the bursts, but not their frequency, increased, raising $[H_2O_2]$ up to 60–80 μM at burst peaks. These observations were made on 2 polyps from 2 specimens (total 4) of *S. pistillata* and *P. damicornis* (**Supplementary Figure 6**).

H_2O_2 had no effect on the swimming activity, or responsiveness to light of *A. salina* even after 24 h in seawater with up to 100 μM of H_2O_2. This suggests that the elevated $[H_2O_2]$ in coral tissues during feeding does not kill zooplankton prey.

Comparison of H_2O_2 Bursts

For each coral species, the strength and duration of the observed H_2O_2 bursts were cataloged and compared between experimental treatments (**Figure 8**). In total, we recorded 352 bursts. Burst strength followed a log-normal distribution and therefore had a high variance.

When comparing the bursts between normal (Light + PS) and inhibited (Light − PS) photosynthesis treatments (**Figure 8**), *S. pistillata* showed a significant increase in both duration and burst strength during the inhibition of photosynthesis compared to normal conditions. *P. damicornis* also showed an increased burst duration but about the same burst strength between the two treatments. The statistical significance for *P. damicornis* was weak due to poor data support (114 vs. 11 observations).

When comparing the bursts observed in the feeding experiment (**Figure 8**) before and after prey capture of prey *S. pistillata* again showed an increased burst duration and strength post-capture. The burst duration pre-capture for *P. damicornis* was anomalously high, likely an artifact, resulting in a significantly lower burst duration post-capture. The burst strength did slightly increase post-capture, but the apparent decrease in burst duration rendered the effective change insignificant. The strongest bursts were observed during the post-capture feeding treatment for both species.

Overall, although the burst properties of each species were affected by our experimental manipulations, both species showed similar burst properties in each setting. Hence we did not observe any inter-specific differences in response to the experimental manipulations.

DISCUSSION

Our H_2O_2 sensors showed rapid and highly linear response to changes in $[H_2O_2]$ up to 50 μM. The H_2O_2 microsensors were fast enough to enable real-time tracking of $[H_2O_2]$ on coral polyps. The H_2O_2 sensors exhibited systemic noise corresponding <200 nM, suggesting that a redesign with might be able to target trace amounts of H_2O_2. The selectivity of the sensor was good, with ascorbate and nitric oxide as the only significant interfering analytes.

The combination of H_2O_2 and O_2 sensors allows us to characterize and measure within the MBL of coral polyps. The small negative values seen in our measurements suggest that the calibration regressions (derived outside the polyp MBL) may be anomalous to apply to measurements made within the coral MBL, particularly in the low range of $[H_2O_2]$ values. The reason for the small offset is not clear but could be caused by stirring sensitivity of sensors or chemical interference due to coral mucus. The $[H_2O_2]$ in close proximity to coral tissue could truly be really lower than any point in our calibration curve as due to antioxidant activity, whereas we assumed that our unamended seawater contained no H_2O_2.

Measurement of H_2O_2 profiles showed that the size of the MBL around the coral polyps was ∼200 μm, which is in the same order of previous studies which measured oxygen and pH (Kühl et al., 1995; de Beer et al., 2000). In our experiments the $[H_2O_2]$ profiles fluctuated often (**Figure 2B**) and even measurements with the sensor placed just outside the MBL showed irregular but frequent large excursions of H_2O_2 levels (data not shown). Such irregular dynamics are likely effects of the vortical flows generated

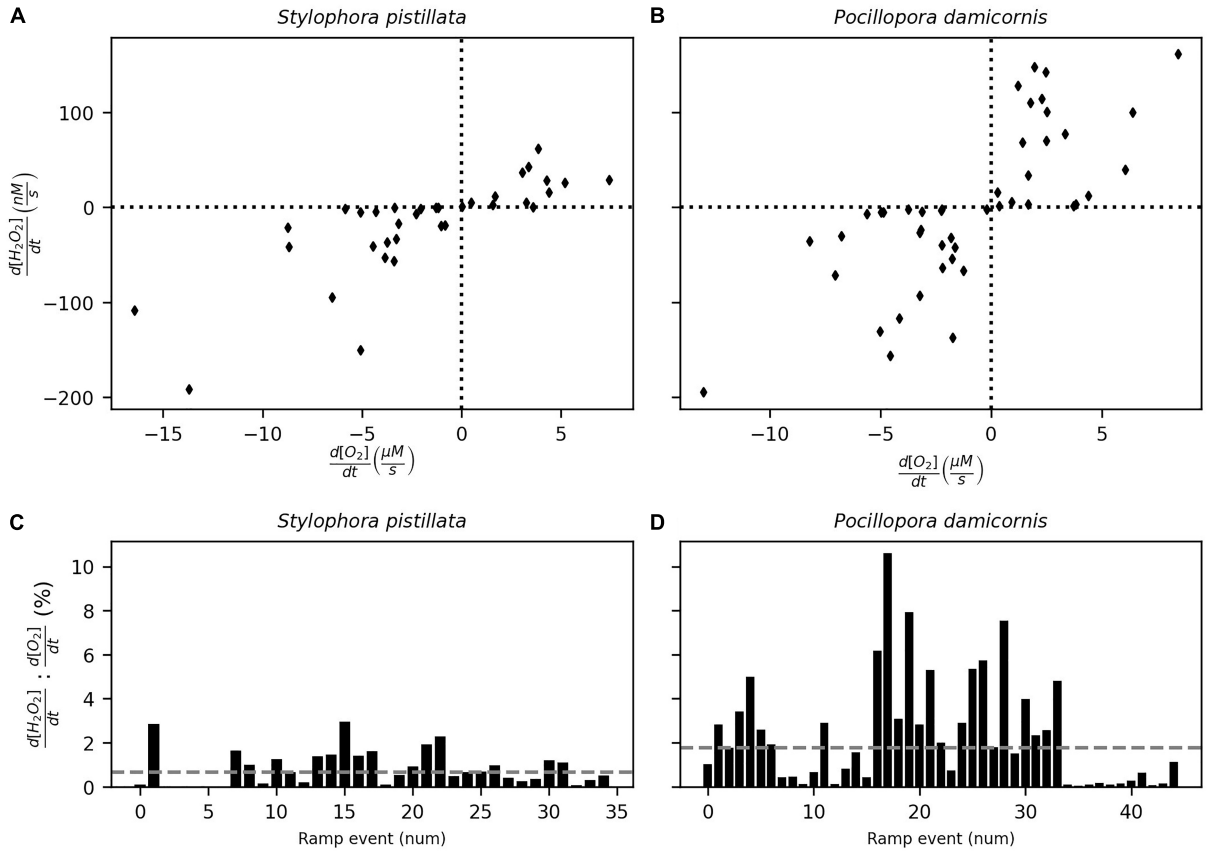

FIGURE 5 | The rates of change of $[O_2]$ and $[H_2O_2]$ on the polyp surface-driven by step changes in incident light for *S. pistillata* **(A)** and *P. damicornis* **(B)**. The ratio (in percentage) between the rates are shown **(C,D)** with the median value (dashed line). $[O_2]$ and $[H_2O_2]$ were measured on adjacent polyps and the rates determined from the initial 30 s of the ramp response (see **Figure 3C**).

by cilia on the coral tissue (Shapiro et al., 2014). Hence, we restricted our measurements to temporal monitoring of $[H_2O_2]$ and $[O_2]$ at the polyp surface. Although the H_2O_2 and O_2 sensor tips could not be co-localized on the same polyp in our setup and thus their signals directly related, we observed correlated signals of $[O_2]$ and $[H_2O_2]$ on adjacent polyps (**Figure 4**).

Across our experiments, we observed two main types of H_2O_2 dynamics at the surface of both coral species: (1) linear H_2O_2 ramps (**Figure 3C**) in immediate response to changes in incident light, and (2) H_2O_2 bursts (**Figure 3B**) that resulted in a short-lived increase of the $[H_2O_2]$. When no bursts occurred, the dynamics of H_2O_2 and O_2 were coupled with the incident light levels (**Figure 4**). The inhibition of photosynthetic activity eliminated the occurrence of light-induced H_2O_2 responses (including ramps), but not of H_2O_2 bursts. The NADH needed to generate these bursts will not be depleted rapidly upon inhibiting photosynthesis. So, bursts occurred unrelated to incident light or photosynthetic activity (**Figure 6**).

It has previously been reported for *Symbiodiniaceae* that the Mehler reaction at the acceptor side of photosystem I (PSI), which reduces O_2 to superoxide with subsequent rapid reduction to H_2O_2 by enzymes in the Mehler Ascorbate Peroxidase pathway, is a prominent alternative electron pathway associated with responses to changes in incident light (Roberty et al., 2014). By using DCMU, we inhibited electron flow through PSII of the *Symbiodiniaceae* by deactivating the plastoquinone pool, leading to the inhibition of oxygen evolution (**Figure 6** and **Supplementary Figures 4**, **5**). H_2O_2 production can also occur in PSII (Pospíšil, 2009) on both the electron donor side (two-electron oxidation of H_2O) and electron acceptor side (one-electron reduction of O_2) of the photo-excited chlorophyll cation P680*, i.e., even when the electron flow through the plastoquinone is blocked through deactivation by DCMU. While other pathways like flavodiiron proteins can reduce O_2 to water without producing H_2O_2 or O_2 (Ilík et al., 2017), these have yet to be identified in *Symbiodiniaceae*. Our observation that addition of DCMU stops the H_2O_2 response to light (coined by us as "ramps") shows that the response is due to photosynthesis related processes. The H_2O_2 ramps in response to illumination changes likely represent a redistribution of electron flow between carbon fixing and photoprotective pathways in the *Symbiodiniaceae* photosystem (Roberty et al., 2014). Our observations indicate that the magnitude of this effect on external H_2O_2 can be 0.01–10% of the change in photosynthesis rate (**Figure 5**). These estimations are under the caveat that peroxide and oxygen concentrations were measured on adjacent polyps.

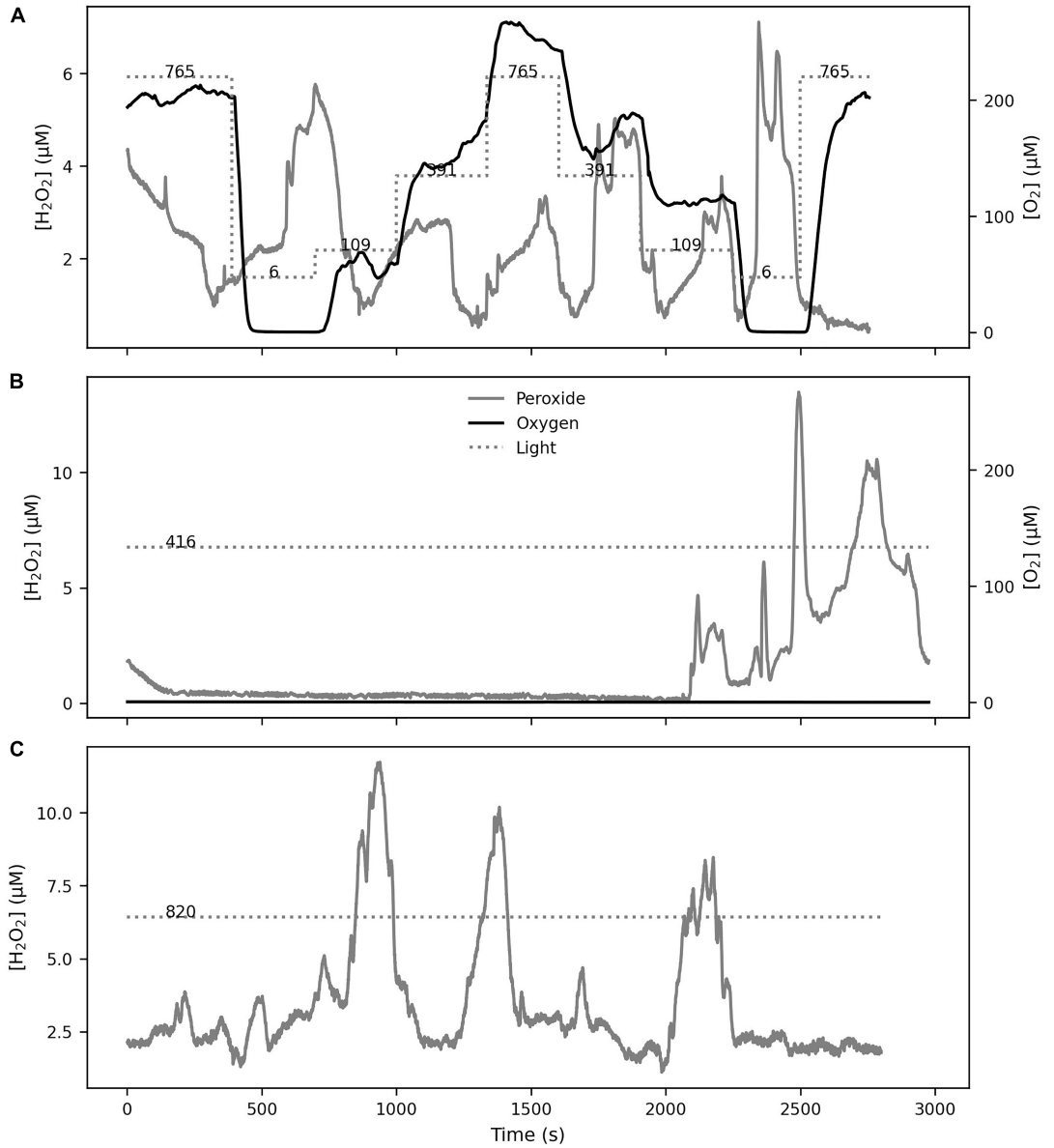

FIGURE 6 | H_2O_2 bursts at the polyp surface occurred independently from incident light or $[O_2]$ levels. Bursts were observed during normal photosynthesis (*S. pistillata* in **A**) as well as during inhibited photosynthesis (*P. damicornis* in **B,C**), showing that the bursts were not induced by changes in incident light or oxygenic photosynthesis.

We recorded remarkably variable and rapid dynamics of H_2O_2 at the polyp surface in our feeding experiments (**Figure 7**). Within 60–100 s of prey capture, the baseline $[H_2O_2]$ increased threefold, indicating that increased respiration by the coral host can drastically change the H_2O_2 level on the coral surface since mitochondrial respiration is a common pathway of ROS formation (Turrens, 2003). The baseline level increase upon prey capture was accompanied by H_2O_2 bursts pushing the momentary $[H_2O_2]$ at the coral surface up to 50–60 μM, which is the highest reported level for corals to our knowledge. Interestingly, H_2O_2 levels as high as 100 μM had no observable direct effect on the *A. salina* in our control measurements, suggesting that the elevated $[H_2O_2]$ has only an indirect effect on the prey, likely through the increased cytotoxicity of the nematocysts (Ayed et al., 2013; Armoza-Zvuloni et al., 2016b) deployed by the corals through exposure to H_2O_2. We observed continued occurrence of H_2O_2 bursts during prey handling by both coral species. Inter-specific variation in ROS production and control by corals has been observed before (Shaked and Armoza-Zvuloni, 2013; Diaz et al., 2016; Ross et al., 2017), but we did not observe a fundamental difference between the two species in their short-term burst dynamics (**Figure 7**).

Bursts of H_2O_2 were a dominant feature of the external H_2O_2 dynamics at the coral surface, occurring in both coral species, independent of light or photosynthetic activity and in conjunction with feeding activity. It must be noted that these

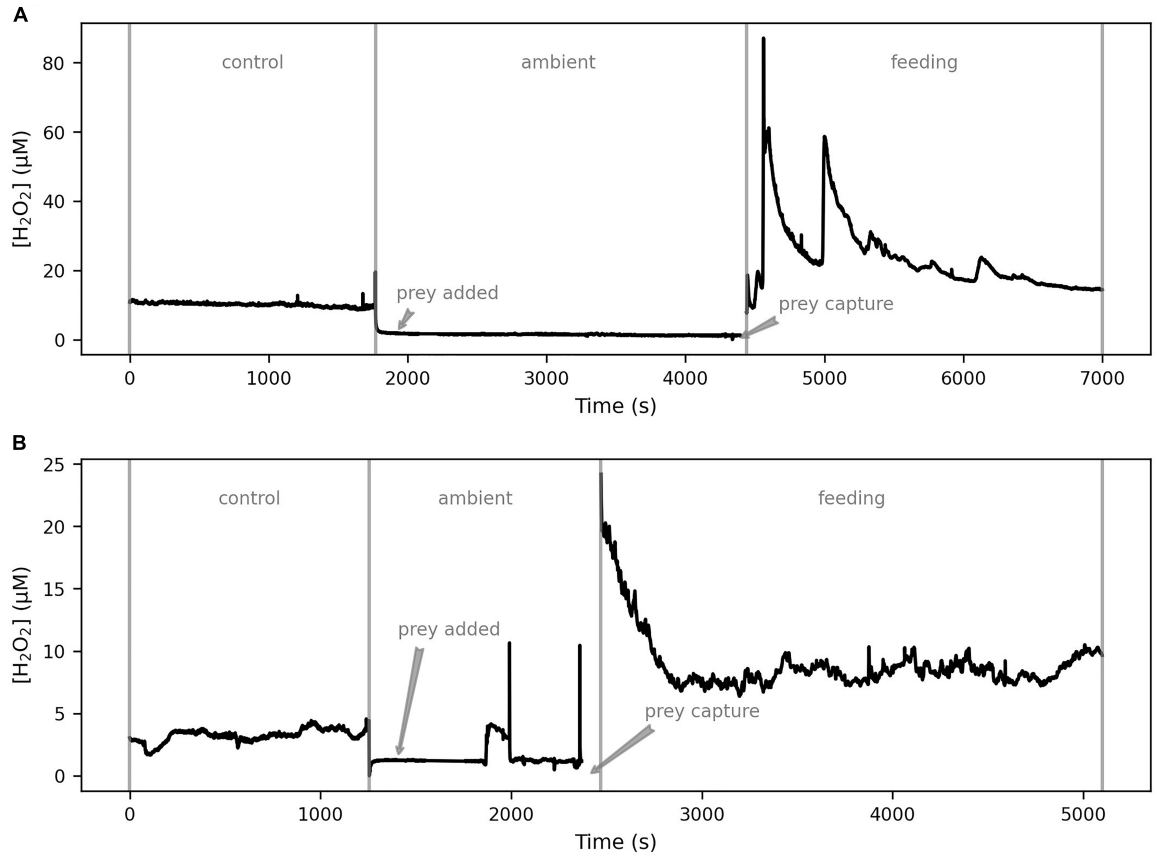

FIGURE 7 | The effects of coral feeding behavior on external H_2O_2 dynamics. With the H_2O_2 sensor positioned on the coral polyp surface, concentrations were measured during the control phase. The sensor was then withdrawn and prey (*A. salina*) were added. On observation of prey capture, the sensor tip was brought back to the polyp surface and monitoring in the feeding phase continued. The two examples (*S. pistillata* in **A** and *P. damicornis* in **B**) show that both species of coral exhibit elevated baseline [H_2O_2] upon prey capture, along with frequent H_2O_2 bursts.

H_2O_2 bursts do not have a natural demarcation due to the continuously modulated ROS level on coral polyps. We used a consistent definition of bursts (see Methods) to be able to parse our time series data to define events of short-term H_2O_2 change. Our analysis of burst properties (**Figure 8**) therefore does not consider the possible correlations between consecutive bursts measured on the same polyp. However, we observed 352 H_2O_2 bursts and the occurrence of bursts was unpredictable, and showed a large variance in the rates of [H_2O_2] change, with values up to 15 $\mu M\ s^{-1}$.

There could be several mechanisms driving the large dynamics of H_2O_2 bursts. Membrane-bound enzymes from the NADPH oxidase and Dual oxidase families are involved in the extracellular generation of ROS (Geiszt et al., 2003; Forteza et al., 2005; Takac et al., 2011), such as Nox1 and Nox2 for superoxide and Nox4, Duox1, and Duox2 for H_2O_2. Given the $\mu M\ s^{-1}$ rates of the H_2O_2 dynamics we observed, we concur with the previous suggestion that it is unlikely that the observed levels of external H_2O_2 in corals are primarily due to dismutation of extracellular superoxide (Armoza-Zvuloni and Shaked, 2014). However, we also observed H_2O_2 bursts under O_2-depleted conditions (**Figures 6B,C**), suggesting that membrane-bound enzymes that reduce O_2 might not be the only viable pathway. Microvesicles, which are small membranous subcellular structures released by cells, are known to be vehicles for delivery of antioxidant and ROS molecules used for the regulation of external ROS levels (Bodega et al., 2019). Microvesicles could be a mechanism for external ROS delivery, typically superoxide which dismutes into H_2O_2, which is decoupled from low-O_2 levels within the coral holobiont (Slauch, 2011). Further investigation is necessary to identify the triggers for H_2O_2 bursts, one possibility being a response to corpuscular pathogenic interactions (Munn et al., 2008; Armoza-Zvuloni et al., 2016a).

Irrespective of the mechanism generating bursts, our study provides evidence that H_2O_2 produced within the coral holobiont is not treated endogenously. We observe that the endosymbiotic algae, due to their photoactivity, are a regular source of H_2O_2 within the coral holobiont. From our observation that H_2O_2 bursts occur even independent of photoactivity, we cannot make a definitive claim about the source of the bursts because the coral host, bacteria, and the algae within the holobiont potentially have oxidase enzymes that can produce ROS bursts. However, our observation that the feeding activity of the coral led to increased baseline and burst levels of H_2O_2 shows that the coral host is also a major source of H_2O_2 in the holobiont.

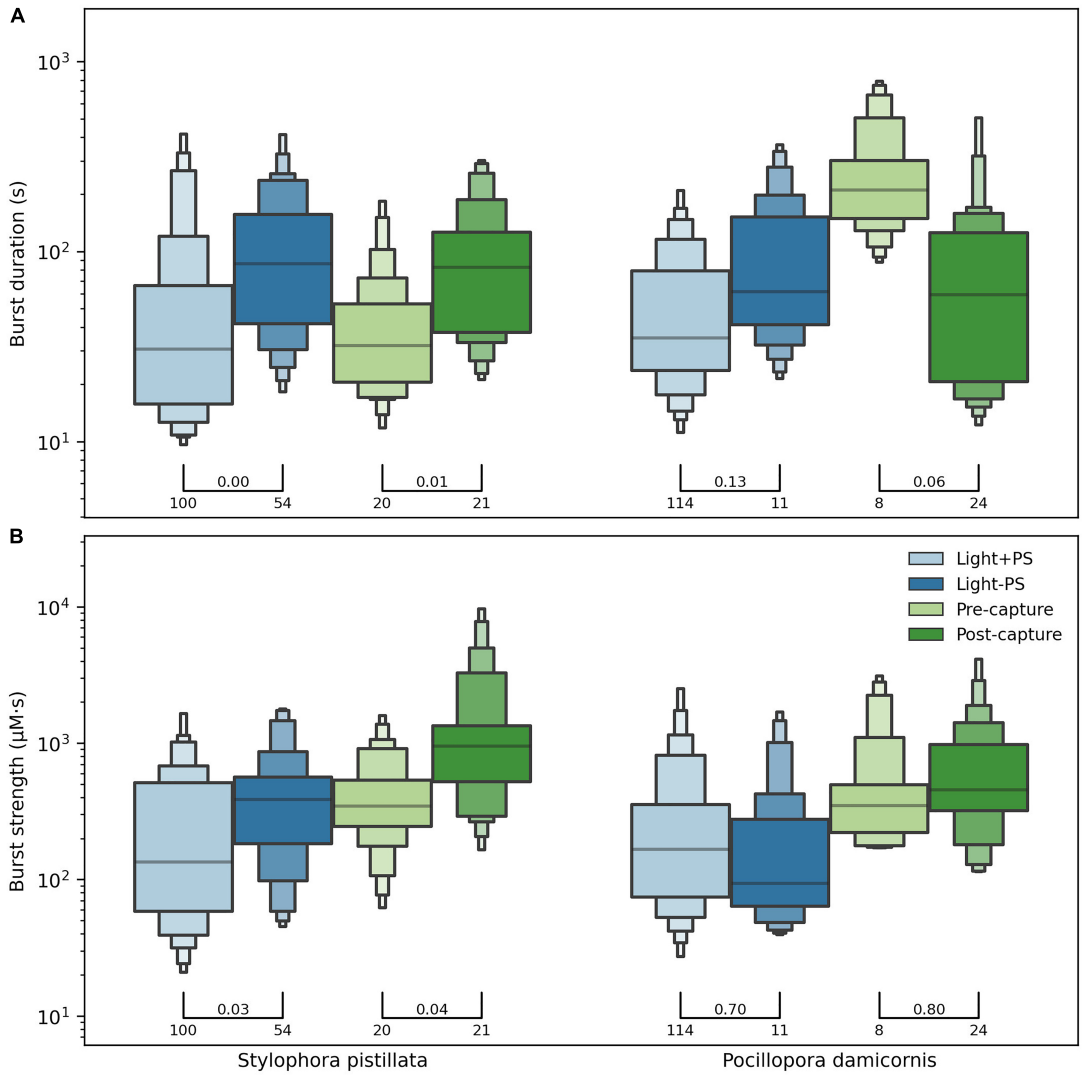

FIGURE 8 | The duration **(A)** and strength **(B)** of H_2O_2 bursts, compared between experimental settings for both coral species. The distribution of values, represented as letter-value plots with horizontal bars for the median value, followed a log-normal distribution (note *y*-axis scale). The *p*-value of Welch's test for difference in group means is indicated above the bars connecting groups, along with the number of bursts in each group. For example, for *S. pistillata* the 100 bursts in the Light + PS and 54 bursts in the Light – PS settings showed a *p*-value of 0.03 when the mean burst strength was compared. Although we saw an effect of our experimental treatments, we did not see an overall significant difference in the burst properties between the two species.

Our observation that H_2O_2 levels on coral polyps during bursts frequently reach 1–6 μM, with short-lived occurrences of 50–60 μM, calls for a redefinition of the "healthy" levels of H_2O_2 in scleractinian corals. This suggests even higher levels of H_2O_2 within the tissue. While this seems implausibly high, it has been shown that H_2O_2 production rates in the μM s^{-1} per cell and steady-state concentrations of millimolar levels can occur (Mittler, 2002). Additionally, cells can transiently generate H_2O_2 levels much higher than steady-state normal conditions (Suzuki et al., 2011) and potentially deliver ROS to extracellular components through microvesicles (Bodega et al., 2019). Further research in identifying the pathways for production and transport of ROS between the intra- and extracellular components of coral tissue is necessary.

Through real-time tracking of H_2O_2 levels on the coral surface, our study reveals that coral tissue is a zone of highly elevated and dynamic H_2O_2 levels, influenced by photosynthetic and feeding activities. Inference of external H_2O_2 signals must not only contend with nM s^{-1} level effect of *Symbiodiniaceae* photosynthesis (in response to illumination changes), but also with the μM s^{-1} level effect of H_2O_2 bursts—suggesting that both "active (regulated)" and "passive (diffusive)" mechanisms are in play (Armoza-Zvuloni and Shaked, 2014). The non-invasive vantage point of microsensors enable observations of such chemical signals with minimal disruption of metabolism or behavior in the holobiont (Sevilgen et al., 2019; Guillermic et al., 2021). However, this external vantage point includes the effects of ROS transport from within the tissue and

hence limits the ability to directly identify or quantify the sources and sinks of ROS within the coral holobiont without targeted experimental controls.

A further consideration in adapting our method to study coral bleaching is that our microsensors were cross-sensitive to nitric oxide. While elevated levels of ROS (at the coral fragment level over 24 h incubation times) have been observed for corals under thermal stress (Franklin et al., 2004; Lesser, 2011), nitric oxide is also produced by the host cnidarian linked to the breakdown of symbiosis that accompanies bleaching (Perez and Weis, 2006). Nitric oxide is also a signaling molecule in the symbiotic algae (Bouchard and Yamasaki, 2008). While our experimental manipulations did not target thermal stress or bleaching, it cannot be excluded as a component of our observed dynamics. Future studies of coral bleaching should consider utilizing peroxide and nitric oxide sensors concurrently.

We recommend further *in situ* studies that achieve high-temporal co-localized measurements of oxygen, hydrogen peroxide and other relevant analytes such as nitric oxide and superoxide in ecophysiological assessments of coral health. The high temporal and spatial resolution are necessary to reveal mechanistic controls and to be integrated into physico-chemical models of the coral microenvironment (Gustafsson et al., 2014; Taylor Parkins et al., 2021). The dynamic nature of ROS plays a vital role in the chemical and behavioral ecology of corals, and further studies are required to disentangle the role of ROS in the health, function, and resilience of corals in reef systems.

DATA AVAILABILITY STATEMENT

The original contributions presented in the study are included in the article/**Supplementary Material**, further inquiries can be directed to the corresponding authors.

AUTHOR CONTRIBUTIONS

AC and SO: conceptualization, data curation, formal analysis, visualization, and writing – original draft. SO: methodology and investigation. AC: software, supervision, and project administration. SO, AC, DB, and SB: writing – review and editing. DB, SB, and AC: resources. DB and AC: funding acquisition. All authors contributed to the article and approved the submitted version.

FUNDING

This work was funded by the institutional budgets of the Max Planck Institute for Marine Microbiology and Leibniz Centre for Tropical Marine Research.

ACKNOWLEDGMENTS

We are grateful for the excellent support with sensor construction and operation provided by the technicians of the Microsensor Group of the Max Planck Institute of Marine Microbiology. Coral samples and handling support was provided by the Marine Experimental Ecology facility of the Leibniz Centre for Tropical Marine Research. We thank Judith M. Klatt (MPIMM) for insightful discussions.

SUPPLEMENTARY MATERIAL

The Supplementary Material for this article can be found online at: https://www.frontiersin.org/articles/10.3389/fmars.2022.812839/full#supplementary-material

REFERENCES

Armoza-Zvuloni, R., and Shaked, Y. (2014). Release of hydrogen peroxide and antioxidants by the coral *Stylophora pistillata* to its external *mileu*. *Biogeosciences* 11, 4587–4598. doi: 10.5194/bg-11-4587-2014

Armoza-Zvuloni, R., Schneider, A., and Shaked, Y. (2016a). Rapid hydrogen peroxide release during coral-bacteria interactions. *Front. Mar. Sci.* 3:124. doi: 10.3389/fmars.2016.00124

Armoza-Zvuloni, R., Schneider, A., Sher, D., and Shaked, Y. (2016b). Rapid Hydrogen Peroxide release from the coral *Stylophora pistillata* during feeding and in response to chemical and physical stimuli. *Sci. Rep.* 6:21000. doi: 10.1038/srep21000

Ayed, Y., Chayma, B., Hayla, A., Abid, S., and Bacha, H. (2013). Is cell death induced by nematocysts extract of medusa *pelagia noctiluca* related to oxidative stress? *Environ. Toxicol.* 28, 498–506. doi: 10.1002/tox.20740

Baird, M. E., Mongin, M., Rizwi, F., Bay, L. K., Cantin, N. E., Soja-Woźniak, M., et al. (2018). A mechanistic model of coral bleaching due to temperature-mediated light-driven reactive oxygen build-up in zooxanthellae. *Ecol. Modell.* 386, 20–37. doi: 10.1016/j.ecolmodel.2018.07.013

Bakus, G. J. (1981). Chemical defense mechanisms on the Great Barrier Reef, Australia. *Science* 211, 497–499. doi: 10.1126/science.7455691

Bodega, G., Alique, M., Puebla, L., Carracedo, J., and Ramírez, R. M. (2019). Microvesicles: ROS scavengers and ROS producers. *J. Extracell. Vesicles* 8:1626654. doi: 10.1080/20013078.2019.1626654

Bouchard, J. N., and Yamasaki, H. (2008). Heat stress stimulates nitric oxide production in symbiodinium microadriaticum: a possible linkage between nitric oxide and the coral bleaching phenomenon. *Plant Cell Physiol.* 49, 641–652. doi: 10.1093/pcp/pcn037

Cronenberg, C., van Groen, B., de Beer, D., and van den Heuvel, H. (1991). Oxygen-independent glucose microsensor based on glucose oxidase. *Anal. Chim. Acta* 242, 275–278. doi: 10.1016/0003-2670(91)87075-I

D'Autréaux, B., and Toledano, M. B. (2007). ROS as signalling molecules: mechanisms that generate specificity in ROS homeostasis. *Nat. Rev. Mol. Cell Biol.* 8, 813–824. doi: 10.1038/nrm2256

de Beer, D., Kühl, M., Stambler, N., and Vaki, L. (2000). A microsensor study of light enhanced Ca2+ uptake and photosynthesis in the reef-building hermatypic coral Favia sp. *Mar. Ecol. Prog. Ser.* 194, 75–85. doi: 10.3354/meps194075

Diaz, J. M., Hansel, C. M., Apprill, A., Brighi, C., Zhang, T., Weber, L., et al. (2016). Species-specific control of external superoxide levels by the coral holobiont during a natural bleaching event. *Nat. Commun.* 7:13801. doi: 10.1038/ncomms13801

Downs, C. A., Fauth, J. E., Halas, J. C., Dustan, P., Bemiss, J., and Woodley, C. M. (2002). Oxidative stress and seasonal coral bleaching. *Free Radic Biol. Med.* 33, 533–543. doi: 10.1016/s0891-5849(02)00907-3

Forteza, R., Salathe, M., Miot, F., Forteza, R., and Conner, G. E. (2005). Regulated hydrogen peroxide production by duox in human airway epithelial cells. *Am. J. Respir. Cell Mol. Biol.* 32, 462–469. doi: 10.1165/rcmb.2004-0302OC

Franklin, D., Hoegh-Guldberg, O., Jones, R., and Berges, J. (2004). Cell death and degeneration in the symbiotic dinoflagellates of the coral *Stylophora pistillata* during bleaching. *Mar. Ecol. Prog. Ser.* 272, 117–130. doi: 10.3354/meps272117

Fridovich, I. (1998). Oxygen toxicity: a radical explanation. *J. Exp. Biol.* 201, 1203–9. doi: 10.1242/jeb.201.8.1203

Geiszt, M., Witta, J., Baff, J., Lekstrom, K., and Leto, T. L. (2003). Dual oxidases represent novel hydrogen peroxide sources supporting mucosal surface host defense. *FASEB J.* 17, 1–14. doi: 10.1096/fj.02-1104fje

Guillermic, M., Cameron, L. P., Corte, I. D., Misra, S., Bijma, J., de Beer, D., et al. (2021). Thermal stress reduces pocilloporid coral resilience to ocean acidification by impairing control over calcifying fluid chemistry. *Sci. Adv.* 7:eaba9958. doi: 10.1126/sciadv.aba9958

Gustafsson, M. S. M., Baird, M. E., and Ralph, P. J. (2013). The interchangeability of autotrophic and heterotrophic nitrogen sources in Scleractinian coral symbiotic relationships: a numerical study. *Ecol. Modell.* 250, 183–194. doi: 10.1016/j.ecolmodel.2012.11.003

Gustafsson, M. S. M., Baird, M. E., and Ralph, P. J. (2014). Modeling photoinhibition-driven bleaching in Scleractinian coral as a function of light, temperature, and heterotrophy. *Limnol. Oceanogr.* 59, 603–622. doi: 10.4319/lo.2014.59.2.0603

Hall, S. B., Khudaish, E. A., and Hart, A. L. (1998). Electrochemical oxidation of hydrogen peroxide at platinum electrodes. Part II: effect of potential. *Electrochim. Acta* 43, 2015–2024. doi: 10.1016/S0013-4686(97)10116-5

Hansel, C. M., and Diaz, J. M. (2021). Production of extracellular reactive oxygen species by marine biota. *Annu. Rev. Mar. Sci.* 13, 177–200. doi: 10.1146/annurev-marine-041320-102550

Ilík, P., Pavlovič, A., Kouřil, R., Alboresi, A., Morosinotto, T., Allahverdiyeva, Y., et al. (2017). Alternative electron transport mediated by flavodiiron proteins is operational in organisms from cyanobacteria up to gymnosperms. *New Phytol.* 214, 967–972. doi: 10.1111/nph.14536

Krueger, T., Hawkins, T. D., Becker, S., Pontasch, S., Dove, S., Hoegh-Guldberg, O., et al. (2015). Differential coral bleaching—Contrasting the activity and response of enzymatic antioxidants in symbiotic partners under thermal stress. *Comp. Biochem. Physiol. A Mol. Integr. Physiol.* 190, 15–25. doi: 10.1016/j.cbpa.2015.08.012

Kühl, M., Cohen, Y., Dalsgaard, T., Jørgensen, B., and Revsbech, N. (1995). Microenvironment and photosynthesis of zooxanthellae in scleractinian corals studied with microsensors for O2, pH and light. *Mar. Ecol. Prog. Ser.* 117, 159–172. doi: 10.3354/meps117159

Lesser, M. P. (2006). Oxidative stress in marine environments: biochemistry and physiological Ecology. *Annu. Rev. Physiol.* 68, 253–278. doi: 10.1146/annurev.physiol.68.040104.110001

Lesser, M. P. (2011). "Coral bleaching: causes and mechanisms," in *Coral Reefs: An Ecosystem in Transition*, eds Z. Dubinsky and N. Stambler (Dordrecht: Springer), 405–419. doi: 10.1007/978-94-007-0114-4_23

Levy, O. (2006). Diel 'tuning' of coral metabolism: physiological responses to light cues. *J. Exp. Biol.* 209, 273–283. doi: 10.1242/jeb.01983

McGinty, E. S., Pieczonka, J., and Mydlarz, L. D. (2012). Variations in reactive oxygen release and antioxidant activity in multiple symbiodinium types in response to elevated temperature. *Microb. Ecol.* 64, 1000–1007. doi: 10.1007/s00248-012-0085-z

Mittler, R. (2002). Oxidative stress, antioxidants and stress tolerance. *Trends Plant Sci.* 7, 405–410. doi: 10.1016/S1360-1385(02)02312-9

Montilla, L., Ramos, R., García, E., and Cróquer, A. (2016). Caribbean yellow band disease compromises the activity of catalase and glutathione S-transferase in the reef-building coral Orbicella faveolata exposed to anthracene. *Dis. Aquat. Org.* 119, 153–161. doi: 10.3354/dao02980

Munn, C. B., Marchant, H. K., and Moody, A. J. (2008). Defences against oxidative stress in vibrios associated with corals: defences against oxidative stress in vibrios. *FEMS Microbiol. Lett.* 281, 58–63. doi: 10.1111/j.1574-6968.2008.01073.x

Mydlarz, L. D., and Jacobs, R. S. (2006). An inducible release of reactive oxygen radicals in four species of gorgonian corals. *Mar. Freshw. Behav. Physiol.* 39, 143–152. doi: 10.1080/10236240600708512

Nathan, C., and Cunningham-Bussel, A. (2013). Beyond oxidative stress: an immunologist's guide to reactive oxygen species. *Nat. Rev. Immunol.* 13, 349–361. doi: 10.1038/nri3423

Paul, V. J., and Puglisi, M. P. (2004). Chemical mediation of interactions among marine organisms. *Nat. Prod. Rep.* 21, 189–209. doi: 10.1039/B302334F

Pawlik, J. R. (1993). Marine invertebrate chemical defenses. *Chem. Rev.* 93, 1911–1922. doi: 10.1021/cr00021a012

Perez, S., and Weis, V. (2006). Nitric oxide and cnidarian bleaching: an eviction notice mediates breakdown of a symbiosis. *J. Exp. Biol.* 209, 2804–2810. doi: 10.1242/jeb.02309

Pospíšil, P. (2009). Production of reactive oxygen species by photosystem II. *Biochim. Biophys. Acta Bioenerg.* 1787, 1151–1160. doi: 10.1016/j.bbabio.2009.05.005

Revsbech, N. P., and Jørgensen, B. B. (1986). "Microelectrodes: their use in microbial ecology," in *Advances in Microbial Ecology*, ed. K. C. Marshall (Boston: Springer), 293–352. doi: 10.1007/978-1-4757-0611-6_7

Roberty, S., Bailleul, B., Berne, N., Franck, F., and Cardol, P. (2014). PSI Mehler reaction is the main alternative photosynthetic electron pathway in Symbiodinium sp., symbiotic dinoflagellates of cnidarians. *New Phytol.* 204, 81–91. doi: 10.1111/nph.12903

Ross, C., Fogarty, N. D., Ritson-Williams, R., and Paul, V. J. (2017). Interspecific variation in coral settlement and fertilization success in response to hydrogen peroxide exposure. *Biol. Bull.* 233, 206–218. doi: 10.1086/696215

Roth, M. S. (2014). The engine of the reef: photobiology of the coral-algal symbiosis. *Front. Microbiol.* 5:422. doi: 10.3389/fmicb.2014.00422

Saragosti, E., Tchernov, D., Katsir, A., and Shaked, Y. (2010). Extracellular production and degradation of superoxide in the coral *stylophora pistillata* and cultured symbiodinium. *PLoS One* 5:e12508. doi: 10.1371/journal.pone.0012508

Sevilgen, D. S., Venn, A. A., Hu, M. Y., Tambutté, E., de Beer, D., Planas-Bielsa, V., et al. (2019). Full in vivo characterization of carbonate chemistry at the site of calcification in corals. *Sci. Adv.* 5:eaau7447. doi: 10.1126/sciadv.aau7447

Shaked, Y., and Armoza-Zvuloni, R. (2013). Dynamics of hydrogen peroxide in a coral reef: sources and sinks. *J. Geophys. Res. Biogeosci.* 118, 1793–1801. doi: 10.1002/2013JG002483

Shapiro, O. H., Fernandez, V. I., Garren, M., Guasto, J. S., Debaillon-Vesque, F. P., Kramarsky-Winter, E., et al. (2014). Vortical ciliary flows actively enhance mass transport in reef corals. *Proc. Natl. Acad. Sci. U. S. A.* 111, 13391–13396. doi: 10.1073/pnas.1323094111

Slauch, J. M. (2011). How does the oxidative burst of macrophages kill bacteria? Still an open question: how do phagocytic ROS kill bacteria? *Mol. Microbiol.* 80, 580–583. doi: 10.1111/j.1365-2958.2011.07612.x

Smith, D. J., Suggett, D. J., and Baker, N. R. (2005). Is photoinhibition of zooxanthellae photosynthesis the primary cause of thermal bleaching in corals? *Glob. Change Biol.* 11, 1–11. doi: 10.1111/j.1529-8817.2003.00895.x

Stanley, G. D., and van de Schootbrugge, B. (2009). "The evolution of the coral–algal symbiosis," in *Coral Bleaching Ecological Studies*, eds M. J. H. van Oppen and J. M. Lough (Berlin: Springer), 7–19. doi: 10.1007/978-3-540-69775-6_2

Sutherland, K. M., Wankel, S. D., and Hansel, C. M. (2020). Dark biological superoxide production as a significant flux and sink of marine dissolved oxygen. *Proc. Natl. Acad. Sci. U. S. A.* 117, 3433–3439. doi: 10.1073/pnas.1912313117

Suzuki, N., Miller, G., Morales, J., Shulaev, V., Torres, M. A., and Mittler, R. (2011). Respiratory burst oxidases: the engines of ROS signaling. *Curr. Opin. Plant. Biol.* 14, 691–699. doi: 10.1016/j.pbi.2011.07.014

Szabó, M., Larkum, A. W. D., and Vass, I. (2020). "A review: the role of reactive oxygen species in mass coral bleaching," in *Photosynthesis in Algae: Biochemical and Physiological Mechanisms Advances in Photosynthesis and Respiration*, eds A. W. D. Larkum, A. R. Grossman, and J. A. Raven (Cham: Springer International Publishing), 459–488. doi: 10.1007/978-3-030-33397-3_17

Takac, I., Schröder, K., Zhang, L., Lardy, B., Anilkumar, N., Lambeth, J. D., et al. (2011). The E-loop is involved in hydrogen peroxide formation by the NADPH Oxidase Nox4. *J. Biol. Chem.* 286, 13304–13313. doi: 10.1074/jbc.M110.192138

Taylor Parkins, S. K., Murthy, S., Picioreanu, C., and Kühl, M. (2021). Multiphysics modelling of photon, mass and heat transfer in coral microenvironments. *J. R. Soc. Interface* 18:20210532. doi: 10.1098/rsif.2021.0532

Tchernov, D., Kvitt, H., Haramaty, L., Bibby, T. S., Gorbunov, M. Y., Rosenfeld, H., et al. (2011). Apoptosis and the selective survival of host animals following thermal bleaching in zooxanthellate corals. *Proc. Natl. Acad. Sci. U. S. A.* 108, 9905–9909. doi: 10.1073/pnas.1106924108

Turrens, J. F. (2003). Mitochondrial formation of reactive oxygen species. *J. Physiol.* 552, 335–344. doi: 10.1113/jphysiol.2003.049478

Weis, V. M. (2008). Cellular mechanisms of Cnidarian bleaching: stress causes the collapse of symbiosis. *J. Exp. Biol.* 211, 3059–3066. doi: 10.1242/jeb.009597

Zhang, T., Diaz, J. M., Brighi, C., Parsons, R. J., McNally, S., Apprill, A., et al. (2016). Dark production of extracellular superoxide by the coral porites astreoides and representative symbionts. *Front. Mar. Sci.* 3:232. doi: 10.3389/fmars.2016.00232

Conflict of Interest: The authors declare that the research was conducted in the absence of any commercial or financial relationships that could be construed as a potential conflict of interest.

Publisher's Note: All claims expressed in this article are solely those of the authors and do not necessarily represent those of their affiliated organizations, or those of the publisher, the editors and the reviewers. Any product that may be evaluated in this article, or claim that may be made by its manufacturer, is not guaranteed or endorsed by the publisher.